Breast Cancer
Vol. 13 No. 1 January 2006

Original Article

Rim Enhancement of Breast Cancers on Contrast-Enhanced MR Imaging: Relationship with Prognostic Factors

Megumi Jinguji[*1,2], Yoriko Kajiya[*2], Kiyohisa Kamimura[*1,2], Masayuki Nakajo[*1], Yoshiaki Sagara[*3], Tetsuya Takahama[*3], Mitsutake Ando[*3], Yoshiaki Rai[*3], Yoshiatsu Sagara[*3], Yasuyo Ohi[*4,5], and Hiroki Yoshida[*5]

*[1]Department of Radiology, Kagoshima University Graduate School of Medical and Dental Sciences, *[2]Department of Radiology, Nanpuh Hospital, *[3]Department of Breast Surgery, Sagara Hospital, *[4]Department of Pathology, Sagara Hospital, *[5]Department of Pathology, Kagoshima University Graduate School of Medical and Dental Sciences, Japan.

Background: There is little evidence regarding associations between magnetic resonance imaging (MRI) features and other important histopathological prognostic factors of breast cancer. The purpose of our study was to investigate the relationship between rim enhancement on MRI and common histopathological prognostic factors of breast cancers.

Methods: We reviewed the contrast-enhanced MR images of 106 consecutive women with histopathologically verified invasive breast carcinomas. Three radiologists assessed the images of each lesion for the presence of rim enhancement on early and delayed images, which were classified into four patterns. Statistical analyses were performed to explore the associations of these patterns with common histopathological prognostic factors and patient age.

Results: Positive ratios of lymph node metastasis and blood vessel invasion and negative ratios of hormone receptors were higher in the invasive cancers with rim enhancement than those without rim enhancement. Rim enhancement was more frequent in invasive ductal cancers with a higher histological grade and larger invasive cancers. The pattern of rim enhancement with centripetal progression showed a significantly increased risk of lymph node metastasis and was associated with a larger size of invasive lesion when compared with the other patterns. Invasive cancers with rim enhancement and little change between the early and delayed images and with centrifugal progression showed significantly less hormone receptor positivity than those without rim enhancement.

Conclusions: Rim enhancement patterns of breast cancers on contrast-enhanced MRI are related to common histopathological prognostic factors and these patterns may be valuable in the preoperative evaluation of breast cancers.

Breast Cancer 13:64-73, 2006.

Key words: Breast cancer, MRI, Rim enhancement, Prognostic factor

Recently, contrast-enhanced magnetic resonance imaging (MRI) has been playing an important part in the detection and estimation of the extent of breast cancer[1-4]. However, the role of contrast-enhanced MRI is still unclear in the evaluation of the biological activity of breast cancer. Rim enhancement is known as a fairly specific sign of breast cancer on contrast-enhanced MRI of breast masses[2,5-7], but it is not always seen in cases of breast cancer. Our goal was to explore the associations between the rim enhancement of invasive breast cancer on dynamic contrast-enhanced MRI and common histopathological prognostic factors used in breast cancer, and to examine whether the rim enhancement patterns are useful in predicting tumor biological activity preoperatively.

Reprint requests to Megumi Jinguji, Department of Radiology, Kagoshima University Graduate School of Medical and Dental Sciences, 8-35-1 Sakuragaoka, Kagoshima, 890-8544, Japan.
E-mail: megu@m.kufm.kagoshima-u.ac.jp

Abbreviations:
MRI, Magnetic resonance imaging; MR, Magnetic resonance; ER, Estrogen receptor; PgR, Progesterone receptor; OR, Odds ratio; CI, Confidence interval; ANOVA, One-way analysis of variance; NPV, Negative predictive value; PPV, Positive predictive value; ROI, Region of interest; PCNA, Proliferating cellular nuclear antigen; VEGF, Vascular endothelial growth factor

Received April 1, 2005; accepted June 15, 2005

Materials and Methods

Patients

We reviewed the magnetic resonance (MR) images of 106 consecutive female patients (age, 27-78 years, mean age 56 years) with histopathologically verified invasive breast carcinomas. After informed consent, they underwent contrast-enhanced dynamic MR mammography before open biopsy and neoadjuvant chemotherapy from April to September 2001. Initially the lesions were detected by physical examination, mammography, or ultrasonography. The histopathologic diagnoses were invasive ductal carcinoma (n = 95) (35 papillotubular carcinomas, 12 solid-tubular carcinomas, 48 scirrhous carcinomas), and others (n = 11) including mucinous carcinoma (n = 6), invasive lobular carcinoma (n = 2), adenoid cystic carcinoma (n = 1), apocrine carcinoma (n = 1), and tubular carcinoma (n = 1).

MR Imaging

MR imaging (MRI) was performed at 1.5 T (Signa; GE Medical Systems, Milwaukee, WI, U.S.A). The tumor-bearing breast in each patient was examined with a dedicated breast coil with the patient in the prone position.

Before administration of contrast material, transverse T1-weighted [500/10 (repetition time msec/echo time msec)] spin-echo imaging and sagittal T2-wighted (4000/84.1) fast spin-echo imaging with fat saturation were performed. The images were obtained using a 32-cm field of view with 9-10-mm thick sections, 2 mm gaps, and a 512 × 224 matrix with two or three signals acquired.

Then dynamic contrast-enhanced images were obtained using a 3D time of flight-first spoiled gradient-recalled echo sequences (7.5/1.7; inversion time 30 msec, flip angle, 15°), a 16-18-cm field of view, 512 × 224 matrix, and 4-6-mm section thickness and no interval gaps. The sagittal or coronal whole breast images were obtained three times, once before and twice after intravenous bolus injection of gadopentetrate dimeglumine (Magnevist; Nihon Schering, Osaka, Japan) at a dose of 0.1 mmol per kilogram of body weight within 10-15 seconds, followed by a 20-mL saline solution flush. The time interval for sequencing was 100 seconds and 300 seconds after administration of contrast agent and each acquisition time was approximately 90 seconds.

Late transverse T1-weighted (850/10) spin-echo imaging with fat saturation was performed after the dynamic study.

Image Analysis

Postprocessing subtraction and black-and-white reversion of dynamic images were performed in all patients. We obtained two different series of subtracted images for each patient. Images obtained before the administration of contrast material were subtracted from early phase (100 seconds) images and delayed phase (300 seconds) images obtained after administration of contrast material, respectively. All subtracted images were assessed by three radiologists (M.J., Y.K., K.K.) together by means of consensus. Contrast medium enhancement on both early and delayed images were classified into "rim" and "entire" patterns. The rim pattern meant that the periphery was more enhanced than the center in a tumor lesion. The "entire" pattern was homogenous enhancement of the tumor. From the changes in the patterns between early and delayed images, four changes in enhancement were observed as follows (Fig 1):

A. Entire enhancement in both early and delayed images. This pattern had no rim enhancement.

B. Rim enhancement in the early image, followed by little change in the delayed image.

C. Rim enhancement in the early image, followed by progressive central filling of contrast medium in the delayed image (centripetal progression of enhancement).

D. Rim enhancement which was clearer in the delayed image than in the early image as a result of central washout of contrast medium (centrifugal progression of enhancement).

In cases of multifocal or multicentric disease showing both entire and rim enhancement patterns, rim enhancement patterns were classified. We visually assessed rim and entire enhancements and changes in the enhancements between early and delayed images. The transverse T1-weighted spin-echo images, sagittal T2-wighted fast spin-echo images and postcontrast T1-weighted spin-echo images after the dynamic study were not used for the study.

Histopathologic Analysis

The histologic materials were stained with

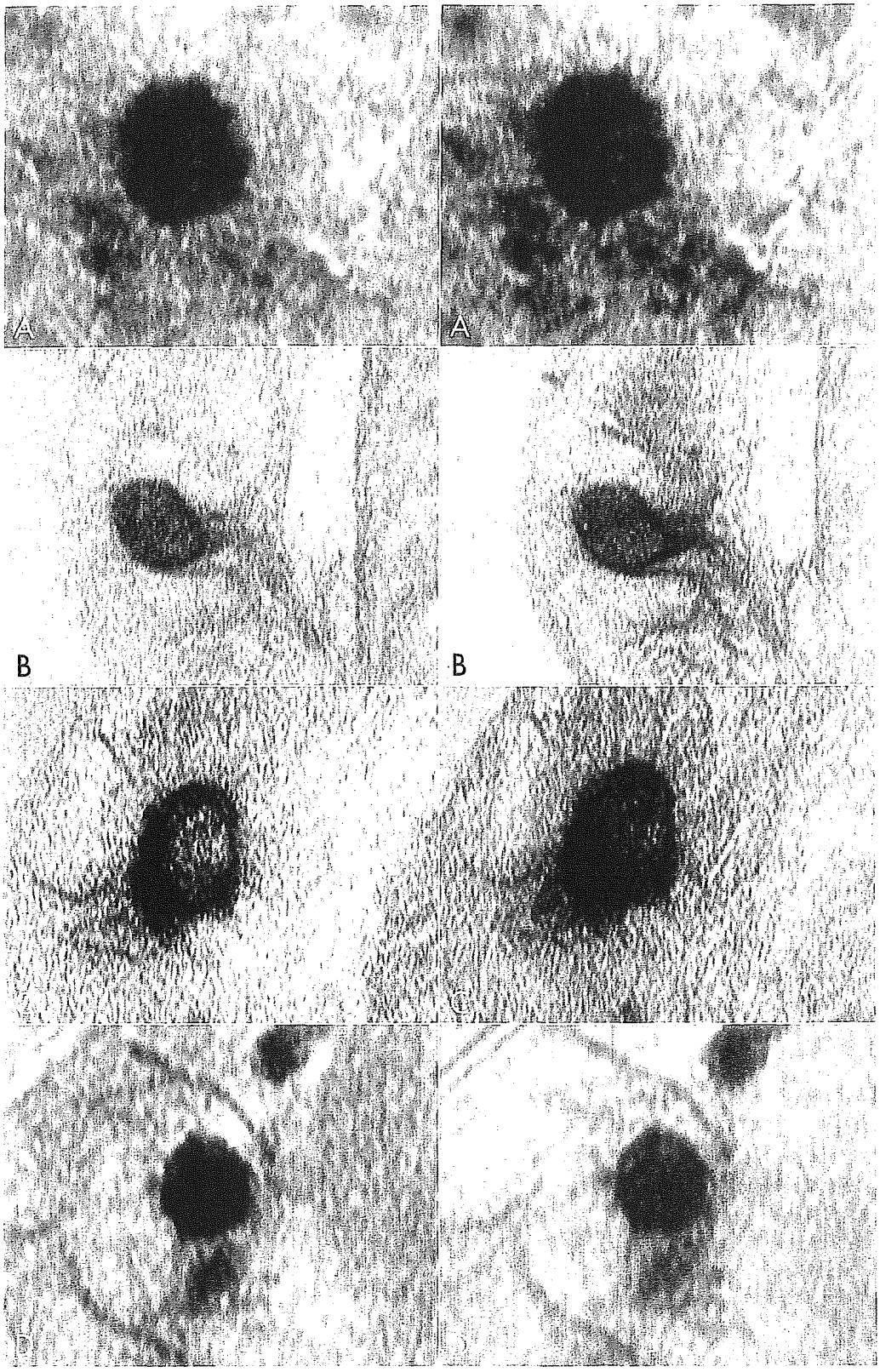

Fig 1. Four patterns changing from early (left) to delayed (right) subtracted and black-and-white reversed 3D-TOF-FSPGR images. (A) Pattern A. Entire enhancement in both early and delayed images. (B) Pattern B. Rim enhancement in the early image, followed by little change in delayed image. (C) Pattern C. Rim enhancement in the early image, followed by progressive central filling of contrast medium in the delayed image. (D) Pattern D. Rim enhancement which was clearer in the delayed image than in the early image as a result of central washout of contrast medium.

hematoxylin and eosin. The histologic interpretations were made by pathologists, without knowledge of the MR imaging findings. All breast cancers were histologically classified according to the criteria of the Japanese General Rules for Clinical and Pathological Recording of Breast Cancer[8]. The histological grade was determined using the modified Bloom and Richardson' criteria[9]. The size of the tumor was microscopically determined as the largest dimension of the invasive lesion in mm. Steroid hormone receptor status was determined by the immunohistochemical analysis. Blood vessel invasion was defined as penetration by the tumor into the lumen of an artery or vein and the presence of blood vessel invasion was recorded. The number of axillary lymph node metastases was recorded.

Immunohistochemical Examination

Tumor specimens were fixed in 10% neutrally buffered formalin and embedded in paraffin. The avidin-biotin-peroxidase method was used for immunohistochemical analysis. Sections 3 μm thick were dewaxed and dehydrated on silanized glass slides. A microwave oven was used for antigen retrieval. Endogenous peroxidase activity was blocked by incubation in hydrogen peroxide. Nonspecific binding was blocked with 10% nonimmune serum. The slides were then incubated in phosphatate-buffered saline with specific monoclonal antibodies, anti-estrogen receptor (1D5, DAKO, Japan) and anti-progesterone receptor (PgR636, DAKO) for 30 min, at room temperature. Normal mouse serum was substituted for primary antibodies as a negative control. Cases were considered estrogen receptor (ER) or progesterone receptor (PgR) positive if nuclear staining appeared in 10% or more of tumor cells.

Statistical Methods

Chi-square test or logistic regression analysis was used to explore the association between rim enhancement and the following prognostic factors: (1) histopathologic type (papillotubular carcinoma, solid-tubular carcinoma, scirrhous carcinoma and others), (2) lymph node metastasis (absence or presence), (3) blood vessel invasion (absence or presence), (4) histological grade (Grades 1-3), (5) invasive size of tumor ($\leqq$20 mm, 21 mm-50 mm and $\geqq$51 mm), (6) ER or PR status (either or both positive and both negative) and (7) patient age ($\leqq$50 and $>$50). Further statistical analyses were performed to explore the associations between the patterns of rim enhancement (A, B, C and D) and prognostic factors in detail. As for hormone receptors, lymph node metastasis and tumor size, odds ratios (ORs) and corresponding 95% confidence intervals (95% CIs) were obtained by logistic regression models using each prognostic factor as a dependent variable. One-way analysis of variance (ANOVA) was used to explore the association of the rim enhancement pattern with tumor size and patient age. Fisher's exact test was used to explore the association between the rim enhancement pattern and blood vessel invasion. A p-value less than 0.05 was considered statistically significant. A statistical program, STATA version 8.1 (STATA Corp., TX, USA), was used.

Results

The association between the presence of rim enhancement and each prognostic factor is summarized in Table 1. Rim enhancement was seen in 55 (52%) of 106 patients with breast cancer. Five factors (lymph node metastasis, blood vessel invasion, histological grade, tumor size and hormone receptor) correlated with rim enhancement, but there was no correlation between rim enhancement and histopathologic type or patient age.

1) The axillary lymph nodes were sampled, and 42 of 105 (40%) patients were found to be positive for metastasis. The positivity rate of lymph node metastasis was significantly higher in the group with rim enhancement ($p=0.017$). Rim enhancement had a 72% (36/50) negative predictive value (NPV) and a 51% (28/55) positive predictive value (PPV) for lymph node metastasis.

2) Rim enhancement had a 100% (51/51) NPV for blood vessel invasion. Although the PPV was 15% (8/55), the association between rim enhancement and blood vessel invasion was statistically significant ($p=0.005$).

3) Histological grading was possible for 95 invasive ductal carcinomas. As the histological grade increased, the rate of rim enhancement became higher ($p<0.001$).

4) As the tumor became larger in size, the rate of rim enhancement became higher ($p<0.001$).

5) The absence of rim enhancement had a 96% (49/51) PPV for the presence of hormone receptors. Although the NPV was 29% (16/55), the association between rim enhancement and hormone receptor was statistically significant ($p<0.001$).

Table 1. Associations Between Rim Enhancement and Prognostic Factors in Breast Cancers

Prognostic factors	Rim enhancement		P-value
	− (%)	+ (%)	
Histopathologic diagnosis			
Papillotubular carcinoma	18 (35)	17 (31)	0.13
Solid-tubular carcinoma	2 (4)	10 (18)	
Scirrhous carcinoma	26 (51)	22 (40)	
Others	5 (10)	6 (11)	
Lymph node metastasis			
Negative	36 (72)	27 (49)	0.017
Positive	14 (28)	28 (51)	
Blood vessel invasion			
Negative	51 (100)	47 (85)	0.005
Positive	0 (0)	8 (15)	
Histological grade			
Grade 1	7 (14)	0 (0)	P for trend < 0.001*
Grade 2	35 (69)	31 (56)	
Grade 3	4 (9)	18 (44)	
Tumor size (mm)			
-20	30 (58)	11 (20)	P for trend < 0.001*
21-50	19 (37)	39 (71)	
51-	2 (4)	5 (9)	
Hormone receptor			
Negative	2 (4)	16 (29)	< 0.001
Positive	49 (96)	39 (71)	
Patient age (years)			
≦ 50	20 (39)	17 (31)	P for trend 0.284*
> 50	31 (61)	38 (69)	

P-values were obtained by chi-square test.
*: P for trend was obtained by logistic regression models using histological grade, tumor size and patient age as continuous variables.

Table 2. Associations Between Enhancement Patterns and Histopathologic Diagnosis in 106 Invasive Carcinomas

Pattern Total (n = 106)	Papillotubular carcinoma (%)	Solid-tubular carcinoma (%)	Scirrhous carcinoma (%)	Other (%)
A (n = 51)	18 (35)	2 (4)	26 (51)	5 (10)
B (n = 20)	7 (35)	8 (40)	3 (15)	2 (10)
C (n = 24)	5 (21)	1 (4)	15 (63)	3 (13)
D (n = 11)	5 (45)	1 (9)	4 (36)	1 (9)

P = 0.002 by chi-square test

Detailed classification of rim enhancement, of 106 patients, pattern A (negative for rim enhancement) was seen in 51 (48%), pattern B in 20 (19%), pattern C in 24 (23%) and pattern D in 11 (10%) patients.

The histopathologic diagnosis according to enhancement pattern was significantly different ($p = 0.002$) (Table 2). For pattern C, scirrhous carcinoma was observed at a higher rate of 63% compared with other histopathologic types. For pattern A, scirrhous carcinoma was also observed at a rate of 51%.

The odds ratio (OR) for lymph node metastasis was significantly increased for pattern C com-

Table 3. Odds Ratios and 95% Confidence Intervals for Lymph Node Metastasis According to Enhancement Patterns

Pattern Total (n = 105)	Lymph node metastasis		OR (95%CI)
	Positive (%)	Negative (%)	
A (n = 50)	14 (28)	36 (72)	1 (referent)
B (n = 20)	8 (40)	12 (60)	1.7 (0.6-5.1)
C (n = 24)	15 (63)	9 (38)	4.3 (1.5-12.0)
D (n = 11)	5 (45)	6 (55)	2.1 (0.6-8.2)

OR, Odds ratio; CI, Confidence interval

Table 4. Associations of Enhancement Patterns and Blood Vessel Invasion in 106 Invasive Carcinomas

Pattern Total (n = 106)	Blood vessel invasion	
	Positive (%)	Negative (%)
A (n = 51)	0 (0)	51 (100)
B (n = 20)	1 (5)	19 (95)
C (n = 24)	6 (25)	18 (75)
D (n = 11)	1 (9)	10 (91)

P = 0.001 by Fisher's exact test

pared to pattern A (OR = 4.3, 95% CI: 1.5-12.0) (Table 3). Multiple logistic regression analysis revealed that this association was not affected by the effects of other prognostic factors.

Pattern C accounted for 6 (75%) of 8 cases with blood vessel invasion. There was a significant difference in the frequency of blood vessel invasion among the four groups of enhancement patterns ($p = 0.001$ by Fisher's exact test) (Table 4). When we limited the analysis to cases with rim enhancement (patterns B, C and D), there was no significant difference in the frequency of blood vessel invasion among the three groups with rim enhancement.

The distribution of histological grade according to the enhancement patterns was statistically different ($p = 0.003$). There was no case of grade 1 cancer among patterns B, C, and D which had rim enhancement. More than half the number of each pattern showed grade 2 (Table 5).

The size of the invasive lesion was categorized into 2 groups, ≤20 mm and >20 mm. The OR for the size of invasive lesion was significantly increased in patterns C (OR = 15.7, 95% CI: 3.3-74.1) and B (OR = 4.3, 95% CI: 1.3-13.6) compared with

Table 5. Associations of Enhancement Patterns and Histological Grade in 95 Invasive Ductal Carcinomas

Pattern Total (n = 95)	Histological grade		
	Grade 1 (n = 7) (%)	Grade 2 (n = 66) (%)	Grade 3 (n = 22) (%)
A (n = 46)	7 (15)	35 (76)	4 (9)
B (n = 18)	0 (0)	9 (50)	9 (50)
C (n = 21)	0 (0)	14 (67)	7 (33)
D (n = 10)	0 (0)	8 (80)	2 (20)

P = 0.003 by chi-square test

pattern A (Table 6). The association between pattern C and the tumor size was not affected by the effects of other prognostic factors, using a multiple logistic regression model. The association between pattern B and tumor size was not significant after adjusting for the effect of hormone receptor status (adjusted OR = 3.2, 95% CI: 0.9-10.9).

The cases with rim enhancement tended to be hormone receptor negative. The OR of hormone receptor positivity was significantly lower for patterns B (OR = 0.06, 95% CI: 0.01-0.3) and D (OR = 0.07, 95% CI: 0.01-0.5) compared with pattern A (Table 7).

There was no significant association between the enhancement patterns and patient age by ANOVA (data not shown).

Discussion

Tumor size, histopathologic type, histological grade, lymph node metastasis, vascular invasion, and hormone receptors are known as prognostic factors of breast cancer, and these prognostic factors contribute to clinical management[10].

The relationships between prognostic factors of breast cancer and contrast-enhanced MRI were recently studied[2, 7, 11-17]. Most studies mainly aimed at the degree of enhancement of breast cancers on MRI to explore the prognostic significance[2, 11-17] while a few papers[7, 11, 12] have described relation between rim enhancement and other prognostic factors of breast cancer.

In 1996, Stomper *et al.*[11] examined the associations between spatial and temporal dynamic MRI enhancement features and DNA S-phase percentages (a measure of cellular proliferative activity) of invasive breast carcinomas (n = 17). They found that increased cell proliferation in invasive cancers

Table 6. Associations Between Enhancement Patterns and Size of Invasive Lesion in 106 Invasive Carcinomas

Pattern Total (n = 106)	Size (mm)			OR (95%CI)
	Mean (SD)	≦ 20 (n = 41) (%)	> 20 (n = 65) (%)	
A (n = 51)	20 (2.1)	30 (73)	21 (32)	1 (referent)
B (n = 20)	28 (2.9)	5 (12)	15 (23)	4.3 (1.3-13.6)
C (n = 24)	35 (2.6)	2 (5)	22 (34)	15.7 (3.3-74.1)
D (n = 11)	31 (8.3)	4 (10)	7 (11)	2.5 (0.6-9.6)
	P = 0.002 by ANOVA			

SD, Standard deviation
OR, Odds ratio; CI, Confidence interval

Table 7. Odds Ratios and 95% Confidence Intervals for Hormone Receptor According to Enhancement Patterns

Pattern Total (n = 106)	Hormone receptor		OR (95%CI)
	Positive (%)	Negative (%)	
A (n = 51)	49 (96)	2 (4)	1 (referent)
B (n = 20)	12 (60)	8 (40)	0.06 (0.01-0.3)
C (n = 24)	20 (83)	4 (17)	0.20 (0.03-1.2)
D (n = 11)	7 (64)	4 (36)	0.07 (0.01-0.5)

OR, Odds ratio; CI, Confidence interval

was significantly associated with a rim enhancement pattern. In 1998, Mussurakis *et al.*[7] determined the presence of rim enhancement by processing the region of interest (ROI) or by assessing subjectively by a reader and they found that there were no significant correlation between rim enhancement (either subjectively or quantitatively) and any of the standard histopathological prognostic factors, including tumor size, differentiation, grade, extensive *in situ* component, lymphovascular invasion, multifocality and multicentricity, and axillary node status, in contrast to our results. We determined the presence of rim enhancement visually but not by processing a ROI. Our visual method to determine the presence of rim enhancement was simple, although the ROI methods may be more objective and reproducible than the visual method. Mussurakis *et al.* also reported that the subjective interpretation of rim enhancement was highly specific but less sensitive in terms of distinguishing cancers from benign lesions compared with the ROI method. Although why the results of associations between rim enhancement and prognostic factors differed between their study and ours is unclear, discrepancies may be due to differences in the pulse sequences used to determine rim enhancement and the number of subjects between their study (n = 64) and ours (n = 106). In 2003, Szabó *et al.*[12] examined the correlation between MR characteristics including rim enhancement and the classical pathologic prognostic factors (tumor size, histologic grade and lymph node status) and immunohistochemically detected biomarkers (c-erbB-2, p53, Ki67, and ER) and reported that the rim enhancement pattern, early maximal enhancement, and washout phenomenon were independently associated with higher histologic grade, positive Ki-67, and negative ER. Our results were similar to theirs in terms of the association between the rim enhancement pattern and higher histologic grade and negative ER status.

There have been some papers which discussed the relationship between prognostic factors of breast cancer and the degree of enhancement on MRI. In 1995, Stomper *et al.*[2] reported that time-intensity curves showed no statistically significant correlations with pathologic size, nodal status, or hormone receptor status of invasive carcinomas. In 1997, Burckley *et al.*[13] reported that correlation between initial enhancement and mean microvessel density was higher in node-positive tumors. In the same year, from the same institute, Mussurakis *et al.*[14] studied the association of the enhancement ratios by ROI analysis with tumor size, histopathological grade, the presence of extensive *in situ* component and lymphovascular invasion, multifocal disease, and axillary lymph node status and showed that there was a strong association

between the enhancement ratios and axillary node status or histological grade. On the other hand, Fischer *et al.*[15] reported that tumor size, tumor grading, axillary lymph nodes showed no significant correlation with the degree of enhancement on dynamic MRI. In 1998, Boné *et al.*[16] reported that there was a significant correlation between contrast enhancement of breast cancer on MRI and both tumor angiogenesis and proliferative cellular activity as shown by proliferating cellular nuclear antigen (PCNA) immunoreactivity and no correlation between contrast enhancement and tumor size, lymph node metastasis, mitotic count or inflammatory response. In 2003, Boné *et al.*[17] reported that multivariate analysis for disease-free survival showed that the signal enhancement ratio and tumor size were significant and independent survival predictors.

There have therefore been various results obtained on the associations between contrast enhanced MRI and prognostic factors, and we have not yet reached a definitive conclusion.

Some investigators have studied the causes of rim enhancement of breast cancers[6, 18]. Buadu *et al.*[6] reported that a high microvessel density in the marginal zone of the viable tumor and/or connective tissues may partly account for the rim pattern of enhancement of breast cancers on MRI. The study by Weidner *et al.* showed that the number of microvesels in the areas of most intensive neovascularization in an invasive breast carcinoma may be an independent predictor of metastatic disease either in axillary lymph nodes or at distant sites (or both)[19] and there have been other reports which showed that the microvessels are located more abundantly at the tumor periphery than the tumor center[13, 18]. Buadu *et al.*[6] reported that early rim enhancement with centripetal progression, which corresponds to pattern C in our study, was fairly specific for carcinomas and seen in invasive carcinomas with a high peripheral and a low central microvessel density, and was associated with central fibrosis and/or necrosis (n = 18; 15 with central fibrosis, 2 with fibrosis and necrosis, and 1 with necrosis alone). In our study, the cases showing pattern C also had a tendency to have much fibrosis. Furthermore, it has been reported that the presence of fibrotic foci is a very useful parameter predicting tumor recurrence and initial distant organ metastasis[20, 21] and centrally necrotizing carcinoma is characterized by early systemic metastasis and an accelerated clinical course[22]. These results appear to explain why the rim enhancement, especially in pattern C, was associated with prognostic factors such as lymph node metastasis and tumor size in our study. Buadu *et al.*[6] reported that among the carcinomas showing early rim enhancement with minimal or no centripetal progression, which corresponds to pattern B in our study, central tumor necrosis was a more common feature than central fibrosis and the central microvessel density was low. The carcinomas with delayed rim enhancement which probably resulted from more rapid central washout of contrast medium, pattern D in our study, were seen to have an expansive growth pattern and tended to have a high marginal microvessel density along with a richly vascularized connective tissue pseudocapsule[6]. We did not measure the microvessel density of our cases and could not find obvious histologic features in either pattern B or D. We speculate that functional differences such as permeability of blood capillaries[23] or physical differences such as pressure of the interstitial components[24] also impact enhancement. In our study, the presence of rim enhancement, especially in patterns B or D, resulted in a significantly lower frequency of hormone receptor positivity. Hormone receptor-negative tumors tend to have low response rates to endocrine therapy[10]. It was reported that absence of tumor necrosis was significantly associated with positive ER[25], that necrosis was significantly associated with low ER levels[26] and elastosis was related to the presence of ER[27-31] and PgR[28, 30, 31]. Therefore, absence of tumor necrosis may result in entire enhancement and partly explain why almost all breast cancers without rim enhancement had hormone receptors. Elastosis may also participate in causing "entire" enhancement, although to our knowledge, there was no report about the relation between elastosis and contrast-enhanced MRI. Matsubayashi *et al.*[18] investigated the histologic basics of rim enhancement of breast masses in detail and reported that small cancer nests, a high ratio of peripheral-to-central microvessel density, peripheral vascular endothelial growth factor (VEGF) expression, and a low ratio of peripheral-to-central fibrosis correlated with early rim enhancement while delayed rim enhancement correlated with a high degree of fibrosis and inflammatory changes.

We compared patterns of rim enhancement in breast cancers with prognostic factors retrospec-

tively. To reveal more clearly the associations between the rim enhancement and various prognostic factors, it is necessary for us to perform a prospective study and multivariate studies for disease-free survival. In addition, the mechanism of rim enhancement of breast cancers have to be clarified.

In summary, rim enhancement of breast cancers on MRI significantly associated with lymph node metastasis, blood vessel invasion, histological grade, tumor size and hormone receptors in our present study. Therefore, the assessment of rim enhancement may be useful for preoperative prediction of prognosis of patients with breast cancer. Contrast-enhanced MRI may offer information not only for loco-regional staging but also for tumor biological activity.

Acknowledgement

We sincerely thank Dr. Chihaya Koriyama for her assistance with the statistical analysis. We also thank Ms. Taeko Kukita, cytologist at Sagara hospital for her help and MRI technologists at Nanpuh hospital for their assistance with data collection.

References

1) Harms SE, Flamig DP, Hesley KL, Meiches MD, Jensen RA, Evans WP, Savino DA, Wells RV: MR imaging of the breast with rotating delivery of excitation off resonance: clinical experience with pathologic correlation. *Radiology* 187:493-501, 1993.
2) Stomper PC, Herman S, Klippenstein DL, Winston JS, Edge SB, Arredondo MA, Mazurchuk RV, Blumenson LE: Suspect breast lesions: findings at dynamic gadolinium-enhanced MR imaging correlated with mammographic and pathologic features. *Radiology* 197:387-395, 1995.
3) Boetes C, Mus RDM, Holland R, Barentsz JO, Strijk SP, Wobbes T, Hendriks JHCL, Ruys SHJ: Breast tumors: comparative accuracy of MR imaging relative to mammography and US for demonstrating extent. *Radiology* 197:743-747, 1995.
4) Orel SG, Schnall MD: MR imaging of the breast for the detection, diagnosis, and staging of breast cancer. *Radiology* 220:13-30, 2001.
5) Hachiya J, Seki T, Okada M, Nitatori T, Korenaga T, Furuya Y: MR imaging of the breast with Gd-DTPA enhancement: comparison with mammography and ultrasonography. *Radiation Medicine* 9:232-240, 1991.
6) Buadu LD, Murakami J, Murayama S, Hashiguchi N, Sakai S, Toyoshima S, Masuda K, Kuroki S, Ohno S: Patterns of peripheral enhancement in breast masses: correlation of findings on contrast medium enhanced MRI with histologic features and tumor angiogenesis. *J Comput Assist Tomogr* 21:421-430, 1997.
7) Mussurakis S, Gibbs P, Horsman A: Peripheral enhancement and spatial contrast uptake heterogeneity of primary breast tumours: quantitative assessment with dynamic MRI. *J Comput Assist Tomogr* 22:35-46, 1998.
8) The Japanese Breast Cancer Society. General rules for clinical and pathological recording of breast cancer, 14th, ed, Kanehara, Tokyo, pp 1-56, 2000.
9) Elston CW, Ellis IO: Pathological prognostic factors in breast cancer. I. The value of histological grade in breast cancer: experience from a large study with long-term follow-up. *Histopathology* 19:403-410, 1991.
10) Elston CW, Ellis IO, Pinder SE: Pathological prognostic factors in breast cancer. *Crit Rev Oncol Hematol* 31:209-223, 1999.
11) Stomper PC, Herman S, Klippenstein DL, Winston JS, Budnick RM, Stewart CC: Invasive breast carcinoma: analysis of dynamic magnetic resonance imaging enhancement features and cell proliferative activity determined by DNA S-phase percentage. *Cancer* 77:1844-1849, 1996.
12) Szabó BK, Aspelin P, Wiberg MK, Tot T, Boné B: Invasive breast cancer: correlation of dynamic MR features with prognostic factors. *Eur Radiol* 13:2425-2435, 2003.
13) Buckley DL, Drew PJ, Mussurakis S, Monson JRT, Horsman A: Microvessel density in invasive breast cancer assessed by dynamic Gd-DTPA enhanced MRI. *J Magn Reson Imaging* 7:461-464, 1997.
14) Mussurakis S, Buckley DL, Horsman A: Dynamic MR imaging of invasive breast cancer: correlation with tumour grade and other histological factors. *Br J Radiol* 70:446-451, 1997.
15) Fischer U, Kopka L, Brinck U, Korabiowska M, Schauer A, Grabbe E: Prognostic value of contrast-enhanced MR mammography in patients with breast cancer. *Eur Radiol* 7:1002-1005, 1997.
16) Boné B, Aspelin P, Bronge L, Veress B: Contrast-enhanced MR imaging as a prognostic indicator of breast cancer. *Acta Radiol* 39:279-284, 1998.
17) Boné B, Szabo BK, Perbeck LG, Veress B, Aspelin P: Can contrast-enhanced MR imaging predict survival in breast cancer? *Acta Radiol* 44:373-378, 2003.
18) Matsubayashi R, Matsuo Y, Edakuni G, Satoh T, Tokunaga O, Kudo S: Breast masses with peripheral rim enhancement on dynamic contrast-enhanced MR images: correlation of MR findings with histologic features and expression of growth factors. *Radiology* 217:841-848, 2000.
19) Weidner N, Semple JP, Welch WR, Folkman J: Tumor angiogenesis and metastasis-correlation in invasive breast carcinoma. *N Engl J Med* 324:1-8, 1991.
20) Colpaert C, Vermeulen P, van Beest P, Goovaerts G, Weyler J, Van Dam P, Dirix L, Van Marck E: Intratumoral hypoxia resulting in the presence of a fibrotic focus is an independent predictor of early distant relapse in lymph node-negative breast cancer patients. *Histopathology* 39:416-425, 2001.
21) Hasebe T, Sasaki S, Imoto S, Mukai K, Yokose T, Ochiai A: Prognostic significance of fibrotic focus in invasive ductal carcinoma of the breast: a prospective observasional study. *Mod Pathol* 15:502-516, 2002.
22) Jimenez RE, Wallis T, Visscher DW: Centrally necrotizing carcinomas of the breast: a distinct histologic subtype with aggressive clinical behavior. *Am J Surg Pathol* 25:331-337, 2001.
23) van Dijke CF, Brasch RC, Roberts TPL, Weidner N, Mathur A, Shames DM, Mann JS, Demsar F, Lang P,

Schwickert HC: Mammary carcinoma model: correlation of macromolecular contrast-enhanced MR imaging characterizations of tumor microvasculature and histologic capillary density. *Radiology* 198:813-818, 1996.
24) Jain RK: Barriers to drug delivery in solid tumors. *Sci Am* 271:42-49, 1994.
25) Fisher ER, Redmond CK, Liu H, Rockette H, Fisher B, collaborating NSABP investigators: Correlation of estrogen receptor and pathologic characteristics of invasive breast cancer. *Cancer* 45:349-353, 1980.
26) Montesco MC, Pluchinotta A, Piffanelli A, Pelizzola D, Giovannini G, Pagnini CA: Hormone receptors and breast cancer: correlations with clinical and histologic features. *Tumori* 70:445-450, 1984.
27) Masters JRW, Sangster K, Hawkins RA, Shivas AA: Elastosis and oestrogen receptors in human breast cancer. *Br J Cancer* 33:342-343, 1976.
28) Rolland PH, Jacquemier J, Martin PM: Histological differentiation in human breast cancer in related to steroid receptors and stromal elastosis. *Cancer Chemother Pharmacol* 5:73-77, 1980.
29) Glaubitz LC, Bowen JH, Cox EB, McCarty KS: Elastotsis in human breast cancer: correlation with sex steroid receptors and comparison with clinical outcome. *Arch Pathol Lab Med* 108:27-30, 1984.
30) Rasmussen BB, Pedersen BV, Thorpe SM, Rose C: Elastosis in relation to prognosis in primary breast carcinoma. *Cancer Res* 45:1428-1430, 1985.
31) Mureşan Z, Duţu R, Voiculetz N: Relationships of steroid hormone receptors, age and histological characteristics in human breast cancer. *Neoplasma* 33:371-377, 1986.

in vivo 20: 33-38 (2006)

Effects of Neonatally-administered 17β-estradiol on Induction of Mammary Carcinomas by 7, 12-Dimethylbenz[*a*]anthracene in Female Rats

MAMORU FUNATO[1,2], HIROAKI KAWAGUCHI[1], TAKAO HORI[1,2], TSUYOSHI YOSHIKAWA[1,2], KENTARO GEJIMA[1], HIDEO KAWASHIMA[1], SYUHEI TAGUCHI[1], KENJIROU NINOMIYA[1], YOSHIHISA UMEKITA[1], RYOICHI NAGATA[2] and HIROKI YOSHIDA[1]

[1]*The Department of Tumor Pathology, Graduate School of Medical and Dental Sciences, Kagoshima University, 8-35-1 Sakuragaoka, Kagoshima 890-8544;*
[2]*Shin Nippon Biochemical Laboratories, Ltd., 2438 Miyanoura, Kagoshima 891-1394, Japan*

Abstract. *Various doses of 17β-estradiol (E_2) were administered subcutaneously to inbred female Sprague-Dawley (SD) rats once at birth. At 50 days after birth, rats in all the groups were given 10 mg of 7, 12-dimethylbenz[a]anthracene (DMBA). In the 1000 μg group, the incidence and number of mammary carcinomas were markedly low, while in the 10 μg group, a large number of mammary carcinomas was noted. Corpora lutea were observed in all rats in the control, 0.1, 1, 10 and 100 μg groups at 50 days old; however, no corpora lutea were observed in any rat in the 1000 mg group at age 50 days and at sacrifice. Observation of the whole-mount specimens showed a low number of terminal end buds (TEBs) in the 1000 μg group and a high number in the 10 μg group. It is suggested that neonatal administration of E_2 affects the gonadotropin-secreting system, resulting in a decrease of progesterone, which is thought to influence the progression of mammary carcinomas induced by DMBA. Moreover, neonatal administration of E_2 directly affects the mammary glands, and it is suggested that E_2 may promote differentiation of TEBs resulting in inhibitory effects on the initiation of mammary carcinomas.*

Mammary carcinoma is on the increase worldwide (1-3), and determination of the cause is essential for its prevention. It is known, both epidemiologically and experimentally, that the development of mammary carcinomas is related to sex hormones, and it must be determined whether substances that act as sex hormones affect the development of mammary carcinomas. It is thought that many environmental endocrine disruptors, particularly during the perinatal or neonatal period, act like sex hormones, directly or indirectly disrupting the reproductive function, thereby inhibiting reproduction (4-6). There is a possibility, therefore, that endocrine-disrupting chemicals might be one of the factors involved in this phenomenon.

It has been shown that a high dose of sex hormones affects the development of rat mammary carcinomas induced by the administration of chemical carcinogens when administered during the neonatal period (7-10).

In the present study, various doses of 17β-estradiol were administered to neonatal female rats at a critical period of morphogenesis and functional development of the mammary glands to examine the effect on 7, 12-dimethyl[*a*]anthracene (DMBA)-induced mammary carcinogenesis.

Correspondence to: Mamoru Funato, D.V.M., M.S., Shin Nippon Biomedical Laboratories, Ltd., 2438 Miyanoura, Kagoshima 891-1394, Japan. Tel: 099-294-2600, Fax: 099-294-3619, e-mail: funato-mamoru@snbl.co.jp

Key Words: Mammary carcinoma, 17β-estradiol, 7, 12-dimethylbenz[a]anthracene, neonatal rats, terminal end buds, corpora lutea.

Materials and Methods

The animals were inbred Sprague-Dawley (SD) female rats, maintained in a filtered air laminar flow at the Division of Laboratory Animal Science, Research Center for Life Science Resources, Kagoshima University, Japan. The rats were given a commercial diet (CE-2, CLEA Inc., Tokyo, Japan) and tap water was available *ad libitum*. The room temperature was maintained at 25°C ± 2°C and relative humidity at 55% ± 10%, with a 12 h-light/dark cycle. The use of animals in this research complied with all the relevant guidelines of the Japanese government and Kagoshima University.

17β-estradiol (E_2, Sigma Chemical Co., St. Louis, MD, USA) at 0.1, 1, 10, 100 and 1000 mg, dissolved in 0.05 ml sesame oil was administered subcutaneously to inbred female SD rats once at birth, while in the control group, 0.05 ml sesame oil, was also administered. At 50 days after birth, all rats were given 10 mg of

0258-851X/2006 $2.00+.40

7, 12-dimethylbenz[*a*]anthracene (DMBA, Wako Pure Chemical Industries Ltd., Osaka, Japan) dissolved in 1 ml sesame oil by gastric intubation. All the rats, except those sacrificed during the observation period, were examined by palpation to detect mammary tumors until the age of 215 to 238 days. All mammary tumors and organs were fixed in 10% phosphate-buffered formalin, dehydrated and embedded in paraffin wax. The widest cut surface was sectioned to 5 mm, stained routinely with H.E. stain and examined histologically. The mean differences were evaluated by *t*-test.

A number of neonatally-treated rats and intact control rats were necropsied at the age of 50 days and the right abdominal mammary glands were collected. These mammary glands were fixed with 10% buffered formalin for 24 h and then stained with alum carmine for 24 h to prepare whole-mount specimens. Terminal end buds (TEBs) were counted from the distal portions of the mammary gland in whole-mounts examined under a stereoscopic microscope.

Ovaries from rats of age 50 days before administration of DMBA and rats sacrificed at the end of the experimental period were collected and examined microscopically.

The mean differences were evaluated by *t*-test. The incidence of tumors and the percentage of rats with corpora lutea were tested by a 4-fold contingency table.

Results

In the 1000 μg group, significantly low numbers of mammary carcinomas per rat and a low incidence of mammary carcinomas were noted compared with the control group. In the 10 mg group, a significantly high number of mammary carcinomas was noted compared with the control group (Table I).

Rats with corpora lutea in the 0.1, 1, 10 and 100 mg groups showed no significant differences in the incidence of mammary carcinomas compared with the control group, although it was not noted (0%) in the 1000 μg group. Observation of the progression of the mammary carcinomas revealed significantly high numbers of mammary carcinomas per rat in the 10 μg group at 200 and 250 days and in the 100 μg group at 200 days, compared with the control group (Tables II and III).

Rats without corpora lutea in the 0.1, 1, 10 and 100 μg groups showed a significantly high incidence of mammary carcinomas compared with the 1000 μg group. Observation of the progression of mammary carcinomas revealed a small number of mammary carcinomas per rat in the 1000 μg group at 150 and 250 days, compared with the 0.1 μg group (Tables II and IV).

At the end of the experimental period, corpora lutea in the ovaries were noted at 79%, 80%, 74% and 55% in the 0.1, 1, 10 and 100 μg groups, respectively. However, no corpora lutea in the ovaries were observed in the 1000 μg group. Significantly low ovary weights were noted in the 1000 μg group compared with the control group at the end of the experimental period. In rats of groups administered 0.1, 1, 10, 100 and 1000 mg E_2 at birth and necropsied at 50 days old, corpora lutea in the ovaries were observed in all rats at up to the 100 μg group, but not in any rat in the 1000 μg group (Tables V and VI).

Table I. *Effects of various dosage levels of E_2 on incidence and number of mammary carcinomas and days of mass detection.*

Group	Number of rats examined	Incidence of mammary carcinomas	Number of carcinomas /rat Mean±SD	Days of mass detection mammary Mean±SD
Control	21	16 (76%)	1.4±1.2	159.0±70.7
17β-estradiol 0.1 μg/body	14	10 (71%)	2.0±2.2	144.2±66.8
17β-estradiol 1 μg/body	15	13 (87%)	2.3±1.8	173.0±59.6
17β-estradiol 10 μg/body	27	24 (89%)	2.4±1.6[a]	164.7±55.8
17β-estradiol 100 μg/body	20	14 (70%)	2.0±2.3	150.2±59.7
17β-estradiol 1000 μg/body	12	3 (25%)[b]	0.3±0.7[b]	157.0±12.5

[a]$p<0.05$: significantly different from the control group
[b]$p<0.01$: significantly different from the control group

Observation of the whole-mount specimens of mammary glands at 50 days revealed a significantly high number of TEBs in the 10 μg group and a significantly low number in the 1000 μg group compared with the control group (Table VI).

Discussion

In the 0.1, 1, 10, 100, and 1000 μg groups, some rats at up to 100 mg showed no corpora lutea in the ovaries at sacrifice, although corpora lutea in the ovaries were observed in all rats in the 0.1, 1, 10 and 100 μg groups at the age of 50 days. Conversely, no corpora lutea in the ovaries were observed in any rat from the 1000 μg group at the age of 50 days or at sacrifice. Moreover, a significant decrease in ovary weight was noted in the 1000 μg group at sacrifice. According to previous studies, this phenomenon is thought to be due to a disturbance of the gonadotropin-secreting system in the hypothalamus from a high dosage of E_2. A high dosage of testosterone propionate during the neonatal period is converted to estrogen in the hypothalamus, resulting in rats without corpora lutea due to disturbance of the gonadotropin-secreting system. We administered 1.25 mg of

Table II. *Effects of various dosage levels of E_2 on incidence of mammary carcinomas and number of mammary carcinoma per rats with/without corpora lutea.*

Group	Number of rats examined	Rats with mammary carcinoma/rats with corpora lutea	Number of mammary carcinomas/rats with corpora lutea	Rats with mammary carcinoma/rats without corpora lutea	Number of mammary carcinomas/rats without corpora lutea
Control	21	16/21 (76%)	1.4±1.2	–	–
17β-estradiol 0.1 μg/body	14	7/11 (64%)	1.6±1.9	3/3 (100%)[a]	2.7±2.9
17β-estradiol 1 μg/body	15	10/12 (83%)	1.8±1.7	3/3 (100%)[a]	3.0±1.0
17β-estradiol 10 μg/body	27	18/20 (90%)	2.4±1.8	6/7 (86%)[a]	1.6±1.3
17β-estradiol 100 μg/body	20	8/11 (73%)	2.3 ±2.4	7/9 (78%)[a]	1.4±1.0
17β-estradiol 1000 μg/body	12	–	–	3/12 (25%)	0.3±0.7

[a]$p<0.05$: significantly different from the 1000 μg group
–: not detected

Table III. *Effect of various dosage levels of E_2 on number of mammary carcinoma per rats with corpora lutea.*

		Number of rats with mammary carcinomas and corpora lutea Number of mammary carcinomas/rats with corpora lutea				
		Day of mass detection				
Group	Number of rats examined	~50[a]	~100[a]	~150[a]	~200[a]	~250[a]
Control	21	1 (4.8%)	7 (33.3%)	11 (52.4%)	11 (52.4%)	16 (76.2%)
		0.05±0.22	0.5±0.8	0.7±0.8	0.8±0.9	1.4±1.2
17β-estradiol	11	1 (9%)	5 (45%)	6 (55%)	7 (64%)	7 (64%)
0.1 μg/body		0.09±0.30	0.6±0.9	1.4±1.9	1.5±1.9	1.6±1.9
17β-estradiol	12	0 (0%)	2 (17%)	5 (42%)	7 (58%)	10 (83%)
1 μg/body		–	0.4±1.0	0.8±1.2	1.3±1.7	1.8±1.7
17β-estradiol	20	0 (0%)	7 (35%)	14 (70%)	15 (75%)	18 (90%)
10 μg/body		–	0.4±0.6	1.1±1.0	1.8±1.5[b]	2.4±1.8[b]
17β-estradiol	11	0 (0%)	5 (45%)	7 (64%)	8 (73%)	8 (73%)
100 μg/body		–	0.8±1.1	1.5±1.4	1.9±1.6[b]	2.3±2.4
17β-estradiol	0	0 (0%)	0 (0%)	0 (0%)	0 (0%)	0 (0%)
1000 μg/body		–	–	–	–	–

[a]Days after birth (approximately days)
[b]$p<0.05$: significantly different from the control group
–: not detected

testosterone propionate to neonatal rats, and those without corpora lutea in the ovaries were administered 20 mg of DMBA at the age of 50 days and were observed for the development of mammary carcinomas. The results of our previous study showed a significant decrease in the number of induced mammary carcinomas (7, 8). Additional administration of progesterone to these rats showed rapid tumorigenesis of mammary carcinomas (9, 11). From the results, it was considered that the tumorigenesis of mammary carcinomas induced by DMBA was suppressed by a long-term decrease in progesterone during the progression period. Accordingly, one cause of marked suppression of mammary carcinoma induction by E_2 in the 1000 μg group in the present study might have been a decrease in progesterone due to the absence of corpora lutea in the ovaries during the progression period of mammary carcinomas. In all rats dosed at 0.1, 1, 10 and 100 μg of E_2, corpora lutea in the ovaries were observed at the age of 50

Table IV. *Effect of various dosage levels of E_2 on number of mammary carcinoma per rats without corpora lutea.*

Group	Number of rats examined	Number of rats with mammary carcinomas and no corpora lutea Number of mammary carcinomas/rats without corpora lutea Day of mass detection ~50[a]	~100[a]	~150[a]	~200[a]	~250[a]
17β-estradiol	3	0 (0%)	1 (33%)	2 (67%)	2 (67%)	3 (100%)
0.1 μg/body		–	0.3±0.6	1.3±1.5	1.3±1.5	2.7±2.9
17β-estradiol	3	0 (0%)	0 (0%)	1 (33%)	1 (33%)	3 (100%)
1 μg/body		–	–	0.3±0.6	0.3±0.6	3.0±1.0
17β-estradiol	7	0 (0%)	2 (29%)	2 (29%)	5 (71%)	6 (86%)
10 μg/body		–	0.3±0.5	0.3±0.5	0.7±0.5	1.6±1.3
17β-estradiol	9	0 (0%)	1 (11%)	2 (22%)	4 (44%)	7 (78%)
100 μg/body		–	0.1±0.3	0.3±0.7	0.7±0.9	1.4±1.0
17β-estradiol	12	0 (0%)	0 (0%)	2/ (17%)	3 (25%)	3 (25%)
1000 μg/body		–	–	0.2±0.4[b]	0.3±0.7	0.3±0.7[b]

[a]Days after birth (approximately days)
[b]$p<0.05$: significantly different from the 0.1 μg/body group
–: not detected

Table V. *Effects of various dosage levels of E_2 on incidence of rats with corpora lutea, and ovary weights.*

Group	Number of rats examined for corpora lutea	Number of rats with corpora lutea	Number of rats for which the ovaries were weighed	Ovary weight (g)/group Mean±SD
Control	21	21 (100%)	14[a]	0.122±0.032
17β-estradiol 0.1 μg/body	14	11 (79%)[b]	14	0.105±0.013
17β-estradiol 1 μg/body	15	12 (80%)[b]	15	0.140±0.029
17β-estradiol 10 μg/body	27	20 (74%)[b]	25[a]	0.128±0.038
17β-estradiol 100 μg/body	20	11 (55%)[c]	20	0.099±0.033
17β-estradiol 1000 μg/body	12	0 (0%)[c]	12	0.058±0.045[c]

[a]Organ weights of animals that died were not weighed
[b]$p<0.05$: significantly different from the control group
[c]$p<0.01$: significantly different from the control group

Table VI. *Effect of various dosage levels of E_2 on the number of terminal end buds (TEBs), and the number of rats with corpora lutea at age of 50 days.*

Group	Number of rats examined	Number of TEBs/rat (Mean±SD)	Rats with corpora lutea
Control	10	46.0±4.6	10 (100%)
17β-estradiol 0.1 μg/body	9	47.3±8.2	9 (100%)
17β-estradiol 1 μg/body	9	42.3±8.4	8 (100%)
17β-estradiol 10 μg/body	10	54.3±9.2[a]	10 (100%)
17β-estradiol 100 μg/body	10	41.0±11.9	10 (100%)
17β-estradiol 1000 μg/body	8	11.8±9.0[b]	0 (0%)[b]

[a]$p<0.05$: significantly different from the control group
[b]$p<0.01$: significantly different from the control group

days; therefore, it was considered that not only a physiological volume of estrogen, but also progesterone, may have been present at the time of carcinogenic exposure to DMBA. It is possible that the progesterone remained for some time during the progression period, resulting in mammary carcinomas that progressed to tumors.

The number of TEBs in the E_2-dosed groups during the neonatal period decreased significantly in the 1000 μg group and increased significantly in the 10 μg group at the age of 50 days. TEBs, undifferentiated terminal ductal structures with a multilayer of highly proliferative epithelial cells, are extremely vulnerable to chemical carcinogenesis (12). The incidence of carcinomas in rodents is directly associated with the density of TEBs in mammary glands at the time of carcinogen administration (12, 13). In response to stimulation from the mammogenic hormones, TEBs differentiate to the more mature structures, namely, alveolar buds (ABs) and lobules

(LOBs), which are less susceptible to carcinogens (12, 14). The progressive differentiation of TEBs into ABs is accentuated by the estrous cycle, which begins at the age of 30-42 days. Development of the mammary gland in non-pregnant females is strongly controlled by the ovary. Ovariectomy can cause regression of the end buds and cessation of growth (15). Since TEBs are considered to be located in the region of the mammary gland most sensitive to DMBA (16, 17), the decreased incidence of mammary carcinomas in the 1000 μg group was thought to have resulted from the decreased number of TEBs seen in this group. A decrease in the number of TEBs noted in the 1000 μg group resulted from rapid differentiation of the mammary glands due to a high dosage of E_2 (unpublished data). The increase in mammary carcinomas noted in the 10 μg group is thought to have been due to increases in the number of TEBs seen in this group, since it is known that the incidence of mammary carcinomas positively correlates with the number of TEBs in the mammary glands of young nulliparous rats at the time of carcinogen exposure (12).

In conclusion, it is suggested that neonatal administration of E_2 affects the gonadotropin-secreting system, resulting in a change in the endocrine system which is thought to influence the progression of mammary carcinomas induced by DMBA. Moreover, neonatal administration of E_2 directly affects the mammary glands, and it is suggested that E_2 may promote the differentiation of TEBs, resulting in inhibitory effects on the initiation of mammary carcinomas. From these results, it is considered necessary that the effects of estrogenic chemicals, such as endocrine-disrupting chemicals, during the neonatal period on the development of mammary carcinomas be further investigated.

Acknowledgements

We are grateful to Mr. T. Kodama, Ms. N. Shirasaka, Ms. Y. Jitoho and Mr. G. Martin for their technical assistance. This work was supported in parts by the Kodama Fund for Medical Research, Japan.

References

1 Yoshida H, Ohi Y, Takasaki T, Kuriwaki K, Honda H, Sato E, Tanaka S, Tokunaga M, Nakamura T and Yoshida N: Sharp increase in the incidence of mammary carcinoma in Kagoshima Prefecture, Japan. Breast Cancer *3*: 9-12, 1996.

2 Martin FL: Genotoxins and the initiation of sporadic breast cancer. Mutagenesis *16*: 155-161, 2001.

3 Wright T and McGechan A: Breast cancer: new technologies for risk assessment and diagnosis. Mol Diagn *7*: 49-55, 2003.

4 Willoughby KN, Sarkar AJ, Boyadjieva NI and Sarkar DK: Neonatally administered tert-octylphenol affects onset of puberty and reproductive development in female rats. Endocrine *26*: 161-168, 2005.

5 Massart F, Seppia P, Pardi D, Lucchesi S, Meossi C, Gagliardi L, Liguori R, Fiore L, Federico G and Saggese G: High incidence of central precocious puberty in a bounded geographic area of northwest Tuscany: an estrogen disrupter epidemic? Gynecol Endocrinol *20*: 92-98, 2005.

6 Safe S: Clinical correlates of environmental endocrine disruptors. Trends Endocrinol Metab *16*: 139-144, 2005.

7 Yoshida H and Fukunishi R: Effect of neonatal administration of sex steroids on 7, 12-dimethylbenz[*a*]anthracene-induced mammary carcinoma and dysplasia in female Sprague-Dawley rats. Gann *69*: 627-631, 1978.

8 Yoshida H, Kadota A, Fukunishi R and Matsumoto K: Induction of mammary dysplasia and mammary carcinoma in neonatally androgenized female rats by 7, 12-dimethylbenz[*a*]anthracene. J Natl Cancer Inst *64*: 1105-1112, 1980.

9 Yoshida H, Fukunishi R, Kato Y and Matsumoto K: Progesterone-stimulated growth of mammary carcinomas induced by 7, 12-dimethylbenz[*a*]anthracene in neonatally androgenized rats. J Natl Cancer Inst *65*: 823-828, 1980.

10 Yoshida H and Huggins C: Effects of neonatally administered-testosterone propionate on the development of target organs of sex hormones and the induction of mammary carcinomas by 7, 8, 12-trimethylbenz (α) anthracene in female Sprague-Dawley rats. Exp Anim *30*: 303-305, 1981.

11 Yoshida H, Kodama A and Fukunishi R: Pathology of early lesions of mammary carcinoma and mammary dysplasia induced by 7, 12-dimethylbenz[*a*]anthracene in neonatally androgenized Sprague-Dawley female rats. Virchows Arch B Cell Path *34*: 33-41, 1980.

12 Russo J and Russo IH: DNA labeling index and structure of the rat mammary gland as determinants of susceptibility to carcinogenesis. J Natl Cancer Inst *61*: 1451-1495, 1978.

13 Russo J, Wilgus G and Russo IH: Susceptibility of the mammary gland to carcinogenesis: differentiation of the mammary gland as determination of tumor incidence and type of lesion. Am J Pathol *96*: 721-736, 1979.

14 Russo J and Russo IH: Biology of disease: biological and molecular bases of mammary carcinogenesis. Lab Invest *57*: 112-137, 1987.

15 Russo IH and Russo J: Mammary gland neoplasia in long-term rodent studies. Environm Health Perspect *104*: 938-967, 1996.

16 Shilkaitis A, Green A, Steele V, Lubet R, Kelloff G and Christov K: Neoplastic transformation of mammary epithelial cells in rats is associated with decreased apoptic cell death. Carcinogenesis *21*: 227-233, 2000.

17 Rowlands JC, Hakkak R, Martin J, Ronin J and Badger TM: Altered mammary gland differentiation and progesterone receptor expression in rats fed soy and whey proteins. Toxicolog Sci *70*: 40-45, 2002.

Received September 28, 2005
Accepted November 14, 2005

CASE REPORT

"End-Stage Kidney" in Longstanding Bulimia Nervosa

Daisuke Yasuhara, MD[1]*
Tetsuro Naruo, MD, PhD[1]
Shuhei Taguchi, MD, PhD[2]
Yoshihisa Umekita, MD, PhD[2]
Hiroki Yoshida, MD, PhD[2]
Shin-ichi Nozoe, MD, PhD[3]

ABSTRACT

Objective: The extent of renal damage over long-term binge/purges has not been well documented in bulimia nervosa (BN).

Method: We describe a 52-year-old woman with longstanding BN subsequent to an 8-year history of anorexia nervosa (AN).

Results: The patient showed chaotic binge/purges and chronic severe hypokalemia after recovery from AN at age 26 years, and renal biopsy showed juxtaglomerular hyperplasia, which was diagnosed as pseudo-Bartter's syndrome. Over the following 26 years, the patient's eating behaviors remained chaotic, and her renal function gradually deteriorated. After the patient died of pneumonia and sepsis at age 52 years, autopsy of her kidney showed chronic interstitial nephritis, proximal tubular swelling, and diffuse glomerular sclerosis, suggesting chronic glomerular injury associated with long-term binge/purges.

Conclusion: To our knowledge, this is the first case report of a patient with BN with long-term binge/purges who developed an eventual "end-stage kidney" characterized by hypokalemic nephropathy and diffuse glomerulosclerosis. © 2005 by Wiley Periodicals, Inc.

(Int J Eat Disord 2005; 38:383–385)

Introduction

Eating disorders, including anorexia nervosa and bulimia nervosa, are commonly seen in adolescents and young females. Particularly for bulimia nervosa, the increasing prevalence rate (1%–2% in 16–35-year-old females) and chronicity after treatment can result in serious social and medical problems (Fairburn & Harrison, 2003; Fairburn, Cooper, Doll, Norman, & O'Connor, 2000). Many medical complications associated with abnormal eating habits exist, including disturbances in gastrointestinal, metabolic, endocrine, and renal function (Fairburn & Harrison, 2003). In particular, renal function has been reported to be impaired even in the short term by severe energy restriction in anorexia nervosa, and by binge/purges in bulimia nervosa (Bock, Cremer, & Werner, 1978; Copeland, 1994; Riemenschneider & Bohle, 1983; Ishikawa et al., 1999; Sharp & Freeman, 1993; Tsuchiya, Nakauchi, Hondo, & Nihei, 1995;). However, little is known about the extent of renal damage over long-term binge/purges. We describe a patient with bulimia nervosa who suffered from longstanding binge/purges and eventual characteristic morphologic changes in her kidney.

Accepted 20 December 2004
Supported by a research grant from the Japanese Ministry of Health, Labor and Welfare.
*Correspondence to: Daisuke Yasuhara, MD, Department of Behavioral Medicine, Kagoshima University Graduate School of Medical and Dental Science, 8-35-1 Sakuragaoka, Kagoshima-City 890-8520, Japan. E-mail: yasuhara@m3.kufm.kagoshima-u.ac.jp
[1] Department of Behavioral Medicine, Kagoshima University Graduate School of Medical and Dental Science, Kagoshima-City, Japan
[2] Department of Tumor Pathology, Course for Advanced Therapeutics, Graduate School of Medical and Dental Science, Kagoshima University, Kagoshima-City, Japan
[3] Department of Clinical Psychology, Faculty of Human Studies, Shigakukan University, Kagoshima, Japan
Published online 17 October in Wiley InterScience (www.interscience.wiley.com). DOI: 10.1002/eat.20198

Case Report

A 26-year-old woman was admitted to our hospital with general fatigue and severe emaciation (body mass index [BMI], 12.8 kg/m^2) in 1975. The patient had no personal history of physical disorders (e.g., diabetes mellitus, hypertension, or renal disease) but she had an 8-year history of anorexia nervosa, binge/purge type (American Psychiatric Association [APA], 1994). On examination, the patient displayed severe hypokalemia (2.0 mmol/L), anemia (hemoglobin level, 7.0 g/dl), and a total protein level of 5.8 g/dl. Blood urea nitrogen (BUN) and serum creatinine concentrations were within normal ranges (BUN level, 10.3 mg/dl; creatinine level, 0.9 mg/dl). However, her creatinine clearance was decreased (58 L/day). Renal biopsy showed no primary or secondary glomerular diseases, but juxtaglomerular hyperplasia, which was diagnosed as pseudo-Bartter's syndrome, was evident. Although

the patient regained weight (BMI, 18.4 kg/m^2) after intensive physical/psychological treatments for 6 months and abnormalities in laboratory studies except for hypokalemia (3.0 mmol/L) were normalized, her binge/purges were unstable and the patient developed bulimia nervosa, purging type (APA, 1994).

After discharge, although the patient maintained normal body weight (BMI > 18.0 kg/m^2) and worked at a local supermarket until age 39 years (1988), her binge/purges were still chaotic. At age 40 years (1989), the patient was referred to our hospital again because of general fatigue, and physical examinations revealed gastroenteritis, esophageal ulcer, hypokalemia (2.5 mmol/L), anemia (hemoglobin level, 8.0 g/dl), and renal insufficiency (BUN level, 46.8 mg/dl; creatinine level, 2.0 mg/dl). Although intensive treatments were applied and her general condition, except for hypokalemia and renal insufficiency, improved, her binge/purges were resistant to treatment and renal impairment gradually worsened (BUN level, 68.0 mg/dl; creatinine level, 5.0 mg/dl, in 1998).

The patient died of pneumonia and sepsis at age 52 years (2001), and autopsy showed bronchopneumonia, gastroenteritis, esophageal ulcer, and bilateral atrophic kidney with multiple cysts (Figure 1). Microscopic examination of the kidney (Figure 2) showed interstitial nephritis (e.g., lymphocytic cellular infiltration), proximal tubular swelling, and diffuse glomerular sclerosis (e.g., atrophy and hyalinized glomeruli). There were no findings relevant to primary or secondary glomerular diseases or juxtaglomerular hyperplasia.

Conclusion

Abnormal eating habits (e.g., severe energy restriction or compensatory binge/purges) have been previously reported to cause renal insufficiency in bulimia nervosa, but were not severe enough to require hemodialysis (Copeland, 1994). However, few studies have revealed the extent of renal damage, especially morphologic changes, over long-term bulimic symptoms (Bock et al., 1978; Copeland, 1994; Riemenschneider & Bohle, 1983; Tsuchiya et al., 1995). To our knowledge, this is the first case report of a patient with longstanding bulimia nervosa and an eventual "end-stage kidney" characterized by hypokalemic nephropathy and diffuse glomerulosclerosis.

Renal insufficiency in eating disorders has been reported to be induced by hypokalemia relevant to vomiting or laxative abuse (Bock et al., 1978; Copeland, 1994; Ishikawa et al., 1999; Riemenschneider & Bohle, 1983; Tsuchiya et al., 1995). The initial biopsy (1977) showed juxtaglomerular hyperplasia, and repeated biopsy (2001) showed interstitial nephritis and proximal tubular swelling. We deem that these morphologic changes were consistent with previous research on hypokalemic nephropathy (Bock et al., 1978; Copeland, 1994; Ishikawa et al., 1999; Riemenschneider & Bohle, 1983; Tsuchiya et al., 1995), and that hypokalemia played an important role in the long-term progress of renal insufficiency in this patient.

Glomerular sclerosis, as seen in our case, appeared to be induced by increased glomerular capillary pressure, glomerular hypertrophy, renal ischemia, and other poorly identified factors relevant to glomerular injury (Marcussen, 1992; Rennke, 1988). In addition to hypokalemia (Bock

FIGURE 1. Bilateral atrophic kidney with multiple cysts.

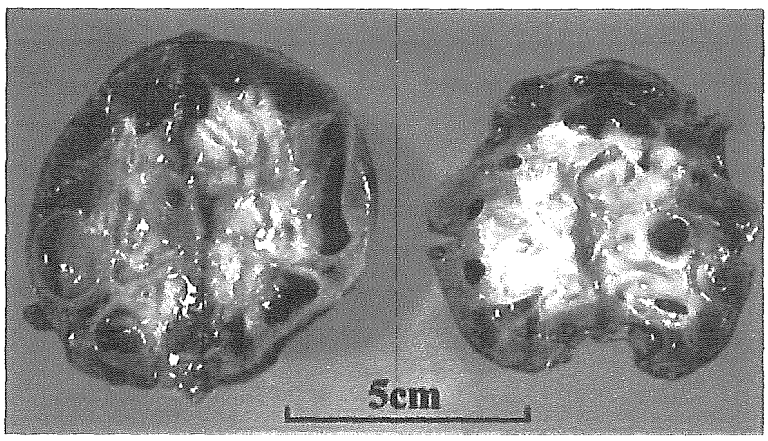

FIGURE 2. (A) Interstitial nephritis and diffuse glomerulosclerosis. (B) Proximal tubular swelling (arrows).

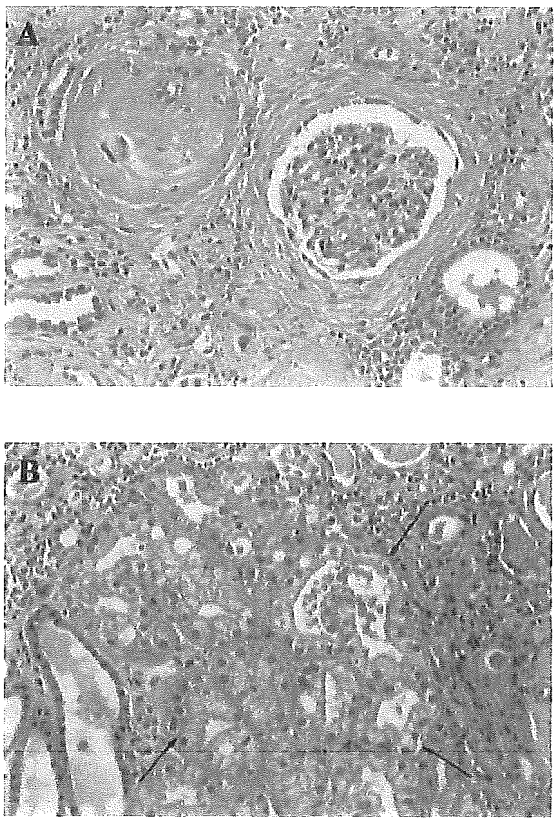

et al., 1978; Copeland, 1994; Ishikawa et al., 1999; Riemenschneider & Bohle, 1983; Tsuchiya et al., 1995), renal insufficiency might be induced by volume depletion relevant to severe energy restriction, vomiting, and laxative abuse in eating disorders (Copeland, 1994). Therefore, we deem that chronic glomerular injury induced by hypokalemia and volume depletion might have resulted in glomerular sclerosis in our patient. Further studies of a larger sample population are needed to investigate the pathogenesis of progressive glomerulosclerosis in bulimia nervosa.

Although physical complications of eating disorders are common, clinicians tend to overlook them (Sharp & Freeman, 1993). Although renal dysfunction in anorexia nervosa appears to be normalized after weight restoration (Boag, Weerakoon, Ginsburg, Havard, & Dandona, 1985), habitual binge/purges in bulimia nervosa tend to be treatment resistant and longstanding (Fairburn & Harrison, 2003; Fairburn et al., 2000), which could lead to irreversible renal changes, as seen in this case. Therefore, our case stresses the importance of early detection, adequate treatment, and intensive monitoring of the physical condition of a patient with bulimia nervosa. Clinicians and bulimic patients themselves should keep in mind the consequences associated with long-term habitual binge/purges.

References

American Psychiatric Association. (1994). Diagnostic and statistical manual of mental disorders (4th ed.). Washington, DC: Author.

Boag, F., Weerakoon, J., Ginsburg, J., Havard, C.W., & Dandona, P. (1985). Diminished creatinine clearance in anorexia nervosa: Reversal with weight gain. Journal of Clinical Pathology, 38(1), 60–63.

Bock, K.D., Cremer, W., & Werner, U. (1978). Chronic hypokalemic nephropathy: A clinical study. Klinische Wochenschrift, 56(Suppl.1), 91–96.

Copeland, P.M. (1994). Renal failure associated with laxative abuse. Psychotherapy and Psychosomatics, 62(3–4), 200–202.

Fairburn, C.G., Cooper, Z., Doll, H.A., Norman, P., & O'Connor, M. (2000). The natural course of bulimia nervosa and binge eating disorder in young women. Archives of General Psychiatry, 57, 659–665.

Fairburn, C.G., & Harrison, P.J. (2003). Eating disorders. Lancet, 361, 407–416.

Ishikawa, S., Kato, M., Tokuda, T., Momoi, H., Sekijima, Y., Higuchi, M., & Yanagisawa, N. (1999). Licorice-induced hypokalemic myopathy and hypokalemic renal tubular damage in anorexia nervosa. International Journal of Eating Disorders, 26(1), 111–114.

Marcussen, N. (1992). Atubular glomeruli and the structural basis for chronic renal failure. Laboratory Investigation, 66(3), 265–284.

Rennke, H.G. (1988). Glomerular adaptations to renal injury or ablation. Role of capillary hypertension in the pathogenesis of progressive glomerulosclerosis. Blood Purification, 6(4), 230–239.

Riemenschneider, T., & Bohle, A. (1983). Morphologic aspects of low-potassium and low--odium nephropathy. Clinical Nephrology, 19(6), 271–279.

Sharp, C.W., & Freeman, C.P. (1993). The medical complications of anorexia nervosa. British Journal of Psychiatry, 162, 452–462.

Tsuchiya, K., Nakauchi, M., Hondo, I., & Nihei, H. (1995). Nephropathy associated with electrolyte disorders. Nippon Rinsho, 53(8), 1995–2000.

Case Report

Acta Haematol

Acta Haematol 2005;113:255–257
DOI: 10.1159/000084679

Received: May 25, 2004
Accepted after revision: October 19, 2004

Fatal Splenic Rupture Caused by Infiltration of Adult T Cell Leukemia Cells

Kosei Arimura[a] Naomichi Arima[b] Toshimasa Kukita[a] Hirosaka Inoue[a]
Akihiko Arai[a] Kakushi Matsushita[a] Shuuhei Taguchi[c] Hiroki Yoshida[c]
Atsuo Ozaki[a] Hideaki Kawada[a] Masaki Akimoto[a] Chuwa Tei[d]

[a]Department of Hematology and Immunology, Kagoshima University Hospital; [b]Division of Host Response, Center for Chronic Viral Diseases; [c]Department of Tumor Pathology, and [d]Department of Cardiovascular, Respiratory and Metabolic Medicine, Graduate School of Medical and Dental Sciences, Kagoshima University, Kagoshima, Japan

Key Words
Splenic rupture · Adult T cell leukemia · Splenomegaly · Infiltration

Abstract
The spleen is an immunological organ commonly involved in both hematological and nonhematological diseases. Pathological rupture of the spleen has been described in a variety of diseases affecting the spleen. Infections have been cited in most cases involving splenic rupture, but are rare in hematological malignancies despite frequent involvement of the spleen. The present report describes a fatal case of splenic rupture caused by infiltration of adult T cell leukemia cells and reports the mechanism of splenic rupture. The importance of rapid diagnosis and surgery is emphasized.

Introduction

Pathological rupture of the spleen has been reported in a large number of diseases [1–4], including infectious mononucleosis [5] and malaria [6]. However, reports of hematological malignancy-induced rupture of the spleen are very rare, despite the frequent involvement of the spleen in such diseases [1–4]. The present report describes a fatal case of splenic rupture caused by infiltration of adult T cell leukemia (ATL) cells.

Case Report

A 53-year-old woman noticed a facial eruption near her nose, and presented to our hospital in 1999. Laboratory examination revealed abnormal lymphocytes comprising 15% of the leukocytes. Serum human T-lymphotropic virus type 1 (HTLV-1) antibody results were positive, while serum lactate dehydrogenase (sLD) levels were within the normal range. Chronic ATL was therefore diagnosed [7]. In June 2002, cervical lymph nodes became swollen and sLD levels were elevated, although the patient displayed no other symptoms. She was admitted to our hospital and treated using combined chemotherapy with biweekly CHOP [8], but treatment was unsatisfactory. In December 2002, ATL cells were increased in peripheral blood, sLD levels were elevated, white blood cell count (WBC) was 63.5 × 10^9/l and sLD level was 9,930 IU/l. After a few days, splenomegaly appeared for the first time since onset, along with sudden and severe anemia, and hemoglobin concentration decreased to 5.0 g/dl. However, no abdominal pain was reported. The patient died from multiple organ failure, and postmortem examination was performed in January 2003.

The spleen weighed 1,236 g, and was greatly enlarged with a 10-cm-long crack apparent along the inferior edge. About 500 ml of bloody ascites was present. Microscopically, diffuse infiltration of ATL cells was observed in the spleen, including the capsule (fig. 1a). The capsule of the spleen was thin due to splenomegaly and partially ruptured (fig. 1b). In another part, ATL cells had pen-

KARGER
Fax +41 61 306 12 34
E-Mail karger@karger.ch
www.karger.com

0001–5792/05/1134–0255$22.00/0

Accessible online at:
www.karger.com/aha

Naomichi Arima, MD, PhD
Division of Host Response, Center for Chronic Viral Diseases
Graduate School of Medical and Dental Sciences, Kagoshima University
Sakuragaoka 8-35-1, Kagoshima, 890-8520 (Japan)
Tel. +81 99 275 5945, Fax +81 99 275 5947, E-Mail nao@m2.kufm.kagoshima-u.ac.jp

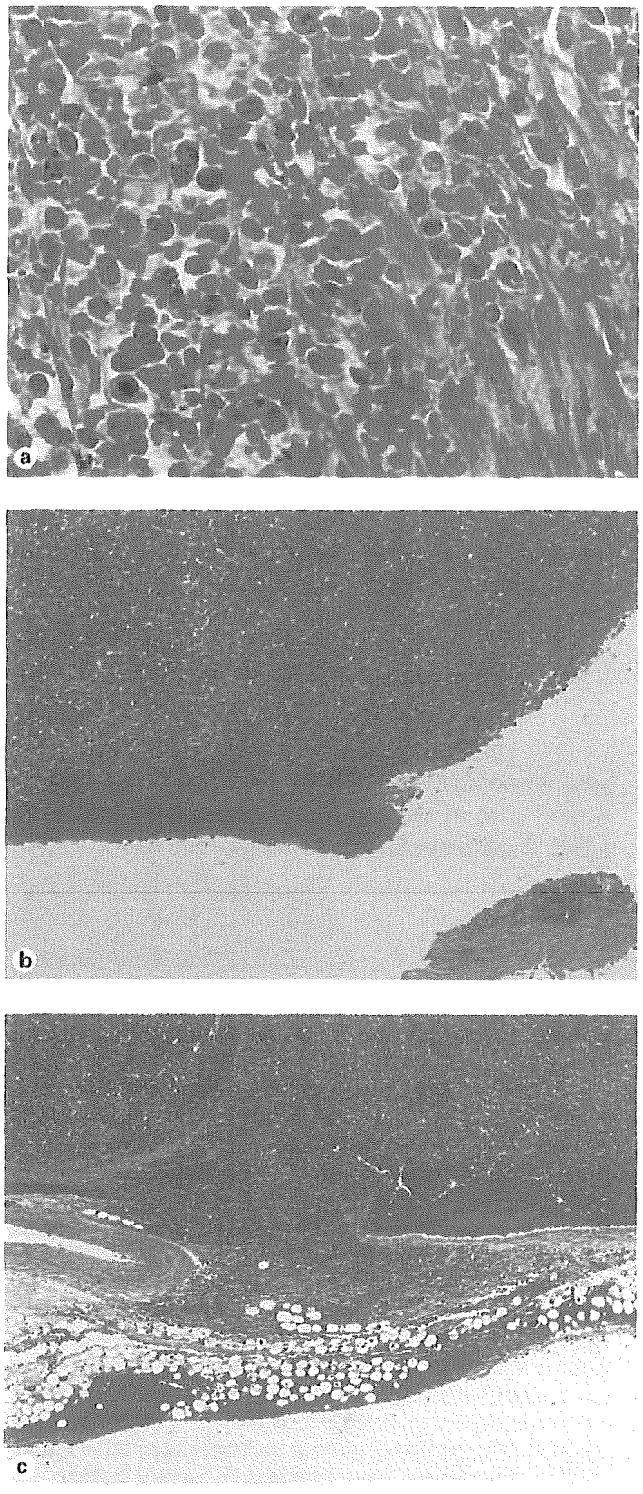

Fig. 1. Pathological findings of spleen. HE. **a** Diffuse infiltration of ATL cells was observed in the spleen, including the capsule. **b** The capsule of the spleen was thin due to splenomegaly and partially ruptured. **c** ATL cells had penetrated the capsule.

etrated the capsule (fig. 1c). Coagulated necrosis and intracapsular bleeding were also apparent. No evidence of infection was identified, including cytomegalovirus, bacteria or fungus. Generalized lymphadenopathy was noted, with pathological infiltration of ATL cells. Infiltration of ATL cells in the heart, lung, liver, kidney, pancreas, uterus, ovary and bone marrow was also found. The stomach and intestines were intact, with no evidence of ATL.

Discussion

The spleen is an immunological organ commonly involved in both hematological and nonhematological diseases. Pathological rupture of the spleen has been associated with a wide variety of underlying conditions, and the phenomenon is uncommon but frequently fatal [9]. While infectious diseases including infectious mononucleosis [5] and malaria [6] have been the most commonly reported disorders associated with splenic rupture, associations with sarcoidosis [10], connective tissue disorders [11, 12] and amyloidosis [13] have also been reported. However, hematological malignancies rarely cause splenic rupture, despite the frequent involvement of the spleen in these diseases [1–4]. This is somewhat surprising, since splenomegaly is a common feature in most hematological diseases, with the spleen sometimes reaching up to 7 kg [3]. Giagounidis et al. [3] reported 136 cases of pathological splenic rupture since 1861, with 34% in acute leukemia, 34% in non-Hodgkin's lymphoma, and 18% in chronic myelogenous leukemia. They also reported higher frequency in males, with a male:female ratio of 3:1, and considerable differences according to specific diseases. Pathological rupture of the spleen has occurred almost exclusively in adults and most ruptured spleens display moderate to severe enlargement [3].

ATL is a hematological malignancy related to HTLV-1 infection. Prognosis in ATL is very poor [7]. The disease is often accompanied by nodal and extranodal lymphomas. In addition, ATL cells often infiltrate into multiple organs, including the spleen [14]. However, reports of pathological rupture of the enlarged spleen in such cases are very rare. Regarding T cell malignancies, only 2 cases of splenic rupture, caused by peripheral T cell lymphoma [2] and mycosis fungoides [15], have previously been reported. To the best of our knowledge, the present report is the first to describe pathological rupture of the spleen due to infiltration of ATL cells.

The precise mechanism of splenic rupture in hematological malignancies is unclear. Recently, Debnath et al. [16] conducted a review that identified 352 cases reported between 1966 and 2000. The spleen is a friable vascu-